3-20-1991

Polarization of Astronomical Maser Radiation

Moshe Elitzur
University of Kentucky, moshe@pa.uky.edu

THE ASTROPHYSICAL JOURNAL, 370:407–418, 1991 March 20

POLARIZATION OF ASTRONOMICAL MASER RADIATION

MOSHE ELITZUR
Department of Physics and Astronomy, University of Kentucky, Lexington, KY 40506-0055
Received 1989 September 15; accepted 1990 September 5

ABSTRACT

The polarization of maser radiation when the source is permeated by an aligned magnetic field is derived for arbitrary angular momenta of the transition states. This generalization is made possible by an analysis of the structure of the propagating waves in a frame aligned with the magnetic axis. The key elements in determining the polarization properties are the assumption of independent and incoherent pump and loss processes for all magnetic sublevels, and the beaming of maser radiation. The radiation propagating in the direction of maximal intensity growth is polarized according to the solutions derived by Goldreich, Keeley, and Kwan for $J = 1 \rightarrow 0$ masers, using various assumptions about the pump rates and the relation between line width and Zeeman splitting. These solutions are shown to be the most general ones for the dominant rays (those propa gating along the longest chords through the source) of steady state beamed masers with arbitrary spins in the relevant domains of parameter space. The beamed nature, and polarization properties, of astronomical maser radiation are established during the unsaturated growth phase, when an increase in overall source dimension results in proportionate tightening of the beaming factor $\Omega/4\pi$.

Subject headings: masers — polarization — radiation mechanisms

1. INTRODUCTION

The radiation of astronomical masers is often polarized (e.g., Reid & Moran 1981; Moran 1989), so an understanding of the conditions that can produce net polarization is important for the study of these sources. The seminal work on this topic is the study by Goldreich, Keeley, & Kwan (1973a, hereafter GKK) of a $J = 1 \rightarrow 0$ maser in a region permeated by an aligned magnetic field. Western & Watson (1984) later extended the GKK method to a $J = 2 \rightarrow 1$ maser when the Zeeman pattern does not develop, and obtained the same results. Because most of the transitions involved in astronomical maser radiation involve spins different from those studied so far, it is important to perform a general analysis, independent of spins. This is the object of this paper, which considers a maser transition between an upper state a and a lower state b with arbitrary angular momenta J_a and J_b, respectively.

For a general analysis of this type it is worthwhile to digress first on the basics of polarization generation. The radiation of a pure wave component is always fully polarized. In an isotropic medium, the spins of the particles—the source of the radiation field—are randomly oriented. As a result, all the individual polarization ellipses are randomly oriented too, and the radiation field is unpolarized. The existence of an overall quantization axis removes the randomness and generally results in net polarization. A common example is the introduction of a magnetic field. This causes precession of the internal magnetic dipoles of the system particles at the rate $g\omega_B$ (g is the Landé factor and ω_B is the radian gyrofrequency) around the magnetic axis. Once this precession rate exceeds all other particle interaction rates, the dipoles can complete a full revolution before being disturbed, the magnetic axis can be considered a good quantization axis, and the sublevels are quantized with respect to it. The requirement that the precession rate exceed all other interaction rates is crucial here. If a molecule collides before completing one gyration, its spin orientation is modified; thus the gyro-rate must exceed the particle collision rate C. Similar depolarization can occur in interaction with photons that may be trapped in optically thick transitions between the maser system and other levels (Goldreich, Keeley, & Kwan 1973b). The interaction rate for a representative IR transition is $B_{IR} J_{IR} = \mathcal{N}_{IR} A_{IR}(1 - \beta_{IR})$, where $\mathcal{N}_{IR}$ ($\simeq 1$) is the appropriate photon occupation number and β_{IR} is the escape probability. Proper space quantization therefore requires

$$g\omega_B > \max [C, \mathcal{N}_{IR} A_{IR}(1 - \beta_{IR})] . \quad (1.1)$$

When this condition is fulfilled, the field provides a good quantization axis, and the magnetic sublevels can be considered oriented with respect to it. This introduces an order in the radiation field and can result in net polarization.

In addition to orienting the spins, the field shifts the energies of the magnetic sublevels in proportion to the m-values, removing their degeneracy. When the field is so strong that the energy shifts exceed the line width, namely, $g\nu_B \gg \Delta\nu$ ($\nu_B = \omega_B/2\pi$), the line splits into a Zeeman pattern. The radiation in each of the Zeeman components is generated in a pure Δm transition, and it is therefore fully polarized. When the magnetic field is only strong enough to order the spins but not to split the line, namely, $g\nu_B \ll \Delta\nu$, the magnetic sublevels can be considered oriented but the Zeeman components fully overlap. Consequently, all the Δm transitions generate radiation at the same unperturbed frequency. Since each Δm transition produces a different type of polarization, the net polarization can be expected to be less than full under these circumstances. It is evident that the degree of polarization will be determined by the relative strengths of the electric fields generated in the different Δm transitions and the interference between them.

This discussion makes it evident that it is advantageous to perform all the calculations in a coordinate frame, which will be called the B-frame, whose z-axis is aligned with the magnetic field, because this is the natural frame for particle interactions. This is the approach taken here. It is the complement of the one taken in the previous studies, where the z-axis was aligned with the direction of wave propagation for all the quantities other than state quantization. The basic relations for the B-frame are derived in § 2, and the equations that govern the level populations and radiative transfer are summarized in

§ 3. The solution for a fully developed Zeeman pattern ($\wp v_B \gg \Delta v$) is derived in § 4, and the solution for overlapping Zeeman components ($\wp v_B \ll \Delta v$) in § 5. The results are summarized and discussed in § 6. To a large extent this section is self-contained and can be read on its own.

It is worthwhile to note that a magnetic field is not the only agent that can define a quantization axis for magnetic sublevels. The same effect is obtained when the system is subject to collisions with a stream of either particles or photons. This situation is analyzed in § 5.3.

2. STOKES PARAMETERS

The introduction of Stokes parameters will follow the discussion of van de Hulst (1957). Consider first a monochromatic plane wave, and denote the direction of the wavevector $\boldsymbol{k}$ as the z-axis. Let some two arbitrary directions perpendicular to $\boldsymbol{k}$ serve as the x- and y-axes. Since the wave's electric field is transverse, it can be written as $\boldsymbol{E} = \mathrm{Re}\,(E_x \boldsymbol{i} + E_y \boldsymbol{i})$, where E_x and E_y are the complex field components. The Stokes parameters are then

$$\begin{aligned} I &= \mathscr{K}(|E_x|^2 + |E_y|^2)\,, \\ Q &= \mathscr{K}(|E_x|^2 - |E_y|^2)\,, \\ U &= \mathscr{K} \times 2\ \mathrm{Re}\,(E_x E_y^*)\,, \\ V &= \mathscr{K} \times 2\ \mathrm{Im}\,(E_x E_y^*)\,, \end{aligned} \tag{2.1}$$

where $\mathscr{K} = (c/8\pi)\delta(\nu - \nu_0)$ is the factor relating field strength to intensity, and ν_0 is the wave frequency. Apart from a sign change of Q the relations here are identical to those employed in GKK.

The field of a pure wave component is always fully polarized, and its polarization parameters obey

$$Q^2 + U^2 + V^2 = I^2\,. \tag{2.2}$$

In a real radiation field the time averaging implied in the definition of the Stokes parameters has two aspects. The first one concerns time averaging over a field configuration with some given values of E_x and E_y at each frequency shift from line center. Time averages involving amplitudes at different frequency shifts are zero, while those involving field amplitudes at the same frequency contribute according to the power spectrum at that frequency, assuming sufficiently large line width (a condition obeyed by astronomical masers; see, e.g., Litvak 1970; GKK). As a result, the δ-function in the coefficient $\mathscr{K}$ is simply replaced with the line profile. This change affects all four Stokes parameters in a similar manner and is unrelated altogether to the degree of polarization. When this phase of the averaging is complete, the Stokes parameters still obey the full-polarization relation of equation (2.2).

The actual polarization of the radiation field is determined when the Stokes parameters are next averaged over all possible field configurations of waves traveling in the same direction with the same intensity profile $I(\nu)$ ($\propto |E_x|^2 + |E_y|^2$), but with different values of E_x and E_y. Because the amplitudes are complex, the equation $|E_x|^2 + |E_y|^2 =$ constant describes the surface of a four-dimensional sphere, and each point on this surface is a radiation field configuration that can be potentially excited and contribute to the actual field. The degree of polarization is determined by the correlations that may or may not exist among all these possible excitations. In an isotropic medium, all configurations are equally likely, and Q, U, and V obviously average out to zero. The vanishing of all three polarization parameters is also evident from the fact that this is the only solution to equations (2.1) invariant under all rotations around z, and the directions of the x- and y-axes are arbitrary in this case.

The situation changes when the radiation is generated in a source with a preferred axis. This will be the case, for example, when the source is permeated by an aligned magnetic field, whose direction will be referred to as the B-axis. The focus of this study is on maser line radiation, generated in transitions between an upper state a and a lower state b with arbitrary angular momenta J_a and J_b, respectively. Each state contains $g_c = 2J_c + 1$ ($c = a, b$) magnetic substates, denoted m and n, respectively. These are quantized along the B-axis when the rate for interaction with the magnetic field exceeds all other relevant microscopic rates, namely, when $\wp\omega_B$ is larger than the collisional and radiative rates (eq. [1.1]). Space quantization introduces a preferred direction in the source, and in general the Stokes parameters need not average out to zero under these circumstances.

Two coordinate frames can then be defined. The z-axis of the first one, the *B-frame*, is defined along the B-axis, and Cartesian components in this frame will be denoted with superscripts. Since $\boldsymbol{B}$ is the quantization axis, all particle interactions correspond to transitions between well-defined states in the B frame and the components of the wave's electric field are generated in specific Δm transitions between the magnetic substates. Thus, if E^0 denotes the electric field generated in $\Delta m = 0$ transitions, then $E^z = E^0$. Likewise, the fields generated in $\Delta m = \pm 1$ transitions produce the two circular components

$$E^{\pm} = 2^{-1/2}(E^x \pm iE^y)\,. \tag{2.3}$$

Therefore, the three components E^p ($p = -1, 0, +1$) generated in $\Delta m = p$ transitions and the corresponding intensities $I^p = \mathscr{K}|E^p|^2$ can be obtained from the transition rates between the various levels, once the population distribution is known.

The second coordinate system, the *k-frame*, is defined by the direction of wave propagation, chosen as its z-axis, which is inclined at an angle θ to the B-axis. Measured quantities obviously correspond to k-frame components of the wave's electric field; those are the ones that enter into the definition of the Stokes parameters. The transformation to the k-frame is straightforward: Select a common y-axis for the two frames. Both x-axes are then in the plane containing $\boldsymbol{B}$ and $\boldsymbol{k}$ and the two frames are related by a simple rotation by angle θ around the common y-axis. Denote the Cartesian components in the k-frame with subscripts; they can then be determined from

$$\begin{aligned} E_x &= E^x \cos\theta + E^z \sin\theta \\ &= 2^{-1/2}(E^+ + E^-)\cos\theta + E^0 \sin\theta\,, \\ E_y &= E^y = -i2^{-1/2}(E^+ - E^-)\,, \\ E_z &= -E^x \sin\theta + E^z \cos\theta \\ &= -2^{-1/2}(E^+ + E^-)\sin\theta + E^0 \cos\theta\,. \end{aligned} \tag{2.4}$$

This simple task, trivial in general, is complicated by the fact that the electric fields of propagating waves must always be orthogonal to the direction of propagation, namely,[1]

$$E_z = 0\,. \tag{2.5}$$

[1] Strictly speaking, it is the longitudinal component of the displacement vector $\boldsymbol{D}$ that should vanish. This distinction can be ignored in astronomical masers.

Although particle interactions can generate three independent field components in the B-frame, the k-frame will always contain only two. The longitudinal component must always be removed, as dictated by this equation; waves that contain a longitudinal electric field do not propagate. This seemingly simple transverse condition is thus a powerful and rather peculiar constraint: Irrespective of the radiation generation mechanisms, no matter what relative strengths of field components the particle interactions tend to produce, whatever the optical depth of the source—this equation must always be obeyed for propagation at any angle.

3. LEVEL POPULATIONS AND RADIATIVE TRANSFER

The system under study involves maser transitions between an upper state a and a lower state b with arbitrary angular momenta J_a and J_b, respectively. Each state contains $g_c = 2J_c + 1$ ($c = a, b$) magnetic substates, denoted m and n, respectively, quantized with respect to the B-axis. The level population equations are obtained from the density matrix of the system; the detailed expressions can be found in Sargent, Lamb, & Fork (1967). Following standard procedures, the steady state level population equations are

$$P_{am} = \Gamma_{am} n_{am} + 3g_a B_{ab} \sum_{p,k} J^p c_p(a, m; b, k)(n_{am} - n_{bk}) ,$$
$$P_{bn} = \Gamma_{bn} n_{bn} - 3g_a B_{ab} \sum_{p,k} J^p c_p(a, k; b, n)(n_{ak} - n_{bn}) . \quad (3.1)$$

Here J^p are the angle averages of I^p, the ensemble-averaged intensities of waves that propagate in the medium in steady state; their fields are thus orthogonal to the direction of propagation. A profile dependence on frequency (corresponding to shifts from line center) is implicitly assumed, so n (units of $\mathrm{cm}^{-3}\ \mathrm{Hz}^{-1}$) are populations per sublevel of particles whose thermal velocities enable them to couple to radiation in the frequency interval $[v, v + dv]$, P_{am} are the pump rates per unit volume and unit frequency interval into the appropriate magnetic substates, and Γ_{am} are the corresponding loss rates. B_{ab} is the Einstein B-coefficient of the $a \rightarrow b$ transition, and the factor $c_p(a, m; b, n)$ is the square of the $3j$ coefficient for vector coupling of (J_a, m), $(1, p)$, and (J_b, n); it enters from the expression for the appropriate matrix element of the dipole moment as derived by the Wigner-Eckart theorem (see, e.g., Messiah 1961). The normalization relations of the c-coefficients, which can be obtained from standard expressions for the $3j$ coefficients, are

$$\sum_{m,n} c_p(a, m; b, n) = 1/3; \quad \sum_{p,m} c_p(a, m; b, n) = 1/g_b;$$
$$\sum_{p,n} c_p(a, m; b, n) = 1/g_a . \quad (3.2)$$

These coefficients ensure that $n = m + p$. In deriving the statistical rate equations, transitions between magnetic substates of the same level, such as $(am) \rightarrow (am')$, for example, were neglected. There is no direct interaction that induces such transitions when quantization is along the magnetic axis. They are generated only in second order, involving transitions to the other level (see Sargent et al. 1967; GKK).

Particle decays generate radiation, and its transfer can be obtained from Maxwell's equations. For a plane wave with frequency v, it follows that

$$\frac{d\boldsymbol{E}}{dl} = \frac{(2\pi)^2 iv}{c} \boldsymbol{P} \quad (3.3)$$

where l measures distances along the propagation direction and $\boldsymbol{P}$ is the volume polarization vector (e.g., GKK; Litvak 1970, 1975; Elitzur 1982). This vector equation applies only to the projection onto the plane perpendicular to the direction of wave propagation, and its transverse k-frame components produce

$$\frac{dE_p E_q^*}{dl} = \frac{(2\pi)^2 iv}{c} (P_p E_q^* - E_p P_q^*) . \quad (3.4)$$

Appropriate components of this tensor relation provide the equations of radiative transfer for the Stokes parameters, which can be written in matrix form

$$\frac{d\boldsymbol{S}}{dl} = \boldsymbol{R} \cdot \boldsymbol{S} , \quad (3.5)$$

where $\boldsymbol{S}$ is the 4-vector (I, Q, U, V) and $\boldsymbol{R}$ is some matrix. The specific form of this matrix depends on the spins involved; for $J = 1 \rightarrow 0$ transitions it can be found in GKK. Alternatively, the transverse fields can be expressed in terms of their components in the B-frame, thus producing a set of equations for the intensity components I^p. The appropriate, rather involved, calculations were performed by Litvak (1975) for arbitrary spins; the intensity components I^q used here are the quantities designated I_{qq} by Litvak. His paper provides the proper spherical harmonics expansion of the intensities of propagating radiation in terms of I^p.

A complete solution of the polarization problem requires solving the coupled set of equations (3.1) for the level populations and (3.5) for the transfer of radiation. This task is further complicated by the fact that the statistical rate equations involve angle-integrated intensities, since the level populations are affected by radiation traveling in all directions. Therefore, in general the radiative transfer equations must be solved for all the rays at every point. However, this difficult problem is greatly simplified in maser sources with sufficient amplification because the radiation is beamed. This point is well illustrated by the simple model in which both levels are assumed scalar. Magnetic subscripts can then be dropped, and the level population equations revert to the often used standard form

$$P_a = \Gamma n_a + B_{ab} J(n_a - n_b) ,$$
$$P_b = \Gamma n_b - B_{ab} J(n_a - n_b) , \quad (3.6)$$

where for further simplification we assume $\Gamma_a = \Gamma_b \equiv \Gamma$. Here J is the angle average of the single intensity I, whose transfer is described by

$$\frac{dI(\mu)}{dl} = \kappa I(\mu) ,$$

where (3.7)

$$\kappa = (hv/4\pi) B_{ab}(n_a - n_b)$$

is the absorption coefficient. The dependence on propagation direction μ is explicitly displayed, and, in principle, all rays must be solved to enable calculation of J. However, in a maser source the intensity always increases with distance traveled, and whatever the geometry, it is impossible for all the rays to have equal lengths. At any given location in a source the ray path length is different in different directions. This is true even in a sphere, the ultimate isotropic structure, at any position other than the center, as illustrated in Figure 1*a*. As a result,

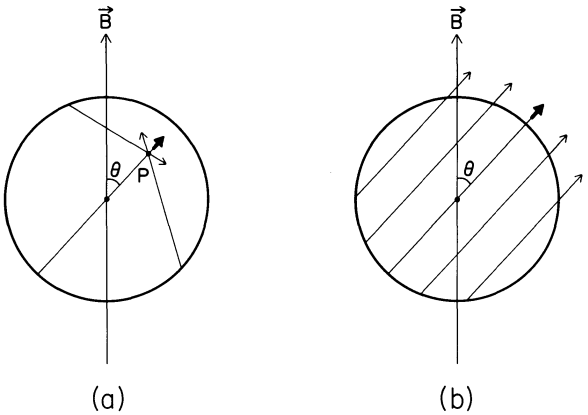

FIG. 1.—Rays in a spherical maser. The dominant rays, those passing through the center, are marked with heavy arrows. (*a*) Some rays at an interior point *P*. (*b*) Rays emitted in the direction inclined at angle θ to the magnetic axis.

maser radiation is highly beamed in all sources with an appreciable gain no matter what their shape, and the angular distribution of the intensity is sharply peaked along the preferred direction of the longest chord through the source. For a given geometrical shape, the beaming angle is determined by the source overall gain; the larger the gain, the more pronounced the beaming (e.g., Elitzur 1990). If the direction of the dominant ray is denoted μ_0, then the angle-averaged intensity obeys

$$J = \frac{\Omega}{4\pi} I(\mu_0) \,. \tag{3.8}$$

where Ω is the solid angle of the radiation beaming pattern. When this relation is inserted in the level population equations (3.6), radiative transfer for the dominant ray becomes

$$\frac{dI(\mu)}{dl} = \frac{1}{2}\frac{h\nu}{\Omega}\left[(P_a - P_b) - \Gamma(n_a - n_b)\right] \,. \tag{3.9}$$

The quantity on the right-hand side is simply the energy radiated into the beaming angle Ω per unit of volume, time, and frequency interval as a result of the net difference between pumping into the maser system and losses to other levels (which can be neglected when the maser saturates). Therefore, $\kappa I(\mu_0)$ is the maser radiation production rate, and the radiative transfer equation for the dominant ray really is not a separate equation with independent contents. Rather, it is simply a statement of energy conservation, since dissipation was neglected—the energy pumped into the system is emitted along the dominant rays. This result can be further understood by transforming into a frame that travels with the radiation. Because the system is in steady state, $dl \to c\,dt$, and the relation between radiative transfer for the dominant ray and the rate of energy supply by the pumping processes, a reflection of the dual role of the term $\kappa I(\mu_0)$, is obvious.

Beaming greatly simplifies radiative transfer for astronomical masers. At every position in the source there exists one, and only one, dominant ray. Different dominant rays do not interact, and the intensity along each one of them can be obtained from considerations of the production of radiation rather than its transfer. From any external observation post the detected radiation is dominated by the emission along the dominant ray pointing at the observer, i.e., the appropriate longest chord through the source, as shown in Figure 1*b* for a spherical maser: radiation emitted along noncentral rays is exponentially weaker and thus can be neglected. A description of the maser radiation field solely in terms of beams centered on dominant rays is appropriate when the overall amplification is appreciable, and the adequacy of this approximation can be estimated from the magnitude of the beaming factor $\Omega/4\pi$; the smaller this factor, the more pronounced the beaming. In the case of an unsaturated sphere of radius R the beaming factor is $1/(4\kappa R)$; in other geometries R is simply replaced by an appropriate linear dimension that characterizes the geometry (e.g., Elitzur 1990). The beaming becomes tighter with increase in radius, and at a modest gain of only $\kappa R = 5$ the beaming factor is already only 5%. When the sphere saturates, the beaming becomes even more pronounced, and, as long as the core does not saturate, the beaming factor varies as $1/(\kappa R)^2$, apart from a weak logarithmic dependence.

The great simplifications in calculating the intensities of dominant rays are a direct reflection of some basic assumptions of maser theory. At every frequency ν across the line width, the dominant ray intensity corresponds to processes associated with that frequency only. The interaction with the maser molecules acts as a frequency filter; correlations between different portions of the frequency bandwidth and fluctuations around the time-averaged solution can be neglected (Litvak 1970; GKK). Similarly, retaining only the beamed radiation and neglecting the isotropic background amounts to a comparable approximation.

Polarization arises from the vector nature of the radiation's electric field, and its description is thus beyond the scope of the simple scalar model. However, taking the vector properties into account does not modify the basic properties of beaming along dominant rays and incoherence across the line width. Because emission along main beams centered on dominant rays is directly related to radiation production, the intensities $I^p(\mu_0)$ can be expected to reflect only pumping into the various p-states, which thus determine the polarization properties of the dominant rays. An important ingredient that does not enter into the analysis of the scalar model is the transverse nature of the propagating waves. The nature of the processes that remove the longitudinal components has never been discussed in the literature, and in that sense the formulation of maser theory is incomplete. Still, whatever the specific removal mechanism, it is important that it not conflict with the basic assumptions that form the foundation for radiative transfer and statistical rate equations. Some standard methods employed in the analysis of laboratory radiation violate those assumptions. For example, a common procedure is to express $m = 0$ photons as linear superpositions of left- and right-circularly polarized photons. This method conflicts with the assumption that the various sublevels are populated independently of each other by incoherent pump and loss processes, and must be applied with care in the analysis of astronomical maser radiation.

4. FULLY RESOLVED ZEEMAN PATTERN: $g\nu_B \gg \Delta\nu$

When the magnetic field is so strong that the gyro-rate exceeds the line width, i.e., $g\nu_B \gg \Delta\nu$ (GKK's case 1), the line splits to a Zeeman pattern and, at a given line frequency, radiation is produced in pure $p = \Delta m$ transitions. Consider an arbitrary position inside such a maser source, assuming that the source is sufficiently large that the radiation is beamed, and consider the intensity $I^p(\mu_0)$ of the dominant ray at a given frequency. This is the strongest intensity at the particular loca-

tion, and only waves with the largest amplitude propagating along μ_0 will contribute to it. Define the real amplitude $E^p = [I^p(\mu_0)/\mathscr{K}]^{1/2}$; then the complex amplitudes of all the propagating waves that contribute to the main beam are of the form

$$E^p e^{ib} . \tag{4.1}$$

Because the waves are produced incoherently, the phases b are random, but they must be real to ensure steady state propagation. Note that any linear combination of complex numbers of the form (4.1) whose overall magnitude is E^p is again such a number, so these amplitudes form a complete set. The ensemble of all propagating waves that contribute to the dominant ray can be generated from these complex amplitudes when b is an arbitrary real number.

Consider now the π-components. These are generated in $\Delta m = 0$ transitions, which produce only the intensity component I^0. From equation (2.4), the transverse components of the propagating waves are therefore

$$\Delta m = 0: \quad E_x = E^0 e^{ib} \sin\theta , \quad E_y = 0 . \tag{4.2}$$

Inserting these components in the definitions of the Stokes parameters (eqs. [2.1]) and performing ensemble average over the random phases b produces

$$\begin{aligned} \Delta m = 0: \quad & I = Q = I^0 \sin^2\theta , \\ & U = V = 0 . \end{aligned} \tag{4.3}$$

These are the Stokes parameters of the dominant rays of π-components.

Consider next the σ-components. These are generated in $\Delta m = \pm 1$ transitions, which produce the intensity components $I^{\pm}$. Similar to the case of the π-components, the transverse components of the propagating waves are

$$\begin{aligned} \Delta m = \pm 1: \quad & E_x = 2^{-1/2} E^{\pm} e^{ib} \cos\theta , \\ & E_y = \mp i 2^{-1/2} E^{\pm} e^{ib} . \end{aligned} \tag{4.4}$$

Again, inserting in the definitions of the Stokes parameters and ensemble-averaging over the phases produces

$$\begin{aligned} \Delta m = \pm 1: \quad & I = \tfrac{1}{2} I^{\pm} (1 + \cos^2\theta) , \\ & Q = -\tfrac{1}{2} I^{\pm} \sin^2\theta , \\ & U = 0 , \\ & V = \pm I^{\pm} \cos\theta , \end{aligned} \tag{4.5}$$

the Stokes parameters of the dominant rays of σ-components.

In deriving the Stokes parameters, the amplitudes of the longitudinal components E_z were ignored because they must vanish for the propagating waves. The removal mechanism for these components remains unspecified, and can be attributed to quantum averaging. Because of the uncertainty principle, two of the three components of the electric field are actually not known, in analogy to the fact that two spin components are completely undetermined when the third is known. Likewise, two of the amplitudes generated in pure Δm transitions are undetermined but average out to zero upon averaging over the precession motions; the assumption that the gyro-rate exceeds all particle interaction rates (eq. [1.1]) is crucial for the adequacy of this averaging (equivalent to the statement that $\boldsymbol{B}$ provides a good quantization axis). The unknown instantaneous fields can be counted upon to secure the transverse condition for propagation at any angle.

The electric fields derived for the ensembles of waves that comprise the dominant rays of various Zeeman components can be inserted in the radiative transfer equation (3.4), Following standard steps, as outlined in Elitzur (1982), for example, the equations of radiative transfer for the intensities $I^p(\mu_0)$ of the dominant rays are simply

$$\frac{dI^p(\mu_0)}{dl} = \kappa^p I^p(\mu_0) , \tag{4.6}$$

where

$$\kappa^p = 3(h\nu/4\pi) g_a B_{ab} \sum_{m,n} c_p(a, m; b, n)(n_{am} - n_{bn}) .$$

The equations were written for the cases in which the Landé factors of the two levels are equal (i.e., $g_a = g_b$ as is the case for OH main lines, for example), so that a number of components contribute at the same frequency. When $g_a \neq g_b$, as is the case for OH satellite lines, each Zeeman component corresponds to a unique pair of magnetic substates (m, n) that can be treated as a separate transition, and the summation over magnetic index m is omitted.

The results show that, similar to the scalar model, the intensities of the dominant rays are directly determined by the radiative interaction terms in the level population equations when the radiation is beamed. Once again, the interaction term $\kappa^p I^p(\mu_0)$ plays a dual role and describes also radiation production, which for the dominant rays becomes radiative transport. While this result may seem obvious, it is in fact highly nontrivial. When a ray corresponds to less than maximal intensity at a given direction, it contains waves whose amplitudes can have different magnitudes, not just different phases, and the ensemble averaging is considerably more involved. From all the rays emanating in the direction θ, the analysis presented above applies only to the dominant ray, marked with a heavy arrow in Figure 1*b*. For arbitrary rays the radiative transfer equations contain off-diagonal terms, and they do not resemble the simple, diagonal form of equation (4.6) for the dominant rays. Therefore, *the dominant rays diagonalize the full set of radiative transfer equations*, a conclusion that can be compared to the solution procedures of GKK for $J = 1 \rightarrow 0$ masers. They derived the explicit form of the full matrix $\boldsymbol{R}$ (eq. [3.5]), including off-diagonal terms, and identified the directions corresponding to maximal unsaturated growth. This procedure led to a diagonalization of the matrix $\boldsymbol{R}$ with the appropriate I^p as the eigenvectors. Indeed, the eigenvalues obtained by GKK are simply $4I/I^p$, and the corresponding Stokes parameters are those derived here. For saturated masers GKK required that the polarization approach a limit, i.e., that the ratios of the Stokes parameters to the intensity I become constant. Again, this is the requirement that the matrix $\boldsymbol{R}$ become diagonal, and the solution is indeed identical to the one obtained in the unsaturated case. The B-frame analysis presented here provides a simple justification for the GKK diagonalization procedures: the dominant rays correspond to the directions of maximal intensity growth, and the radiative transfer equations are diagonal for these rays. The solutions obtained here are in complete agreement with the GKK results; indeed, they provide an explicit construction of the GKK solutions and extend them from $J = 1 \rightarrow 0$ to arbitrary spins.

Polarization is a natural extension of other characteristic properties of the dominant rays, namely, that their radiation corresponds to incoherent pumping across the frequency bandwidth and inside the beaming cone. The exactness of both of these properties has a statistical nature that improves with

increases in source size and averaging times. Similarly, dominant-ray radiation produced in the polarization p-state interacts only with particles in magnetic sublevels separated by $\Delta m = p$. This is an exact, rather than statistical, symmetry property, owing to the discrete nature of the dipole selection rules. As a result, the polarization properties emerge at once when beaming becomes an adequate description of the emitted radiation; the Stokes parameters derived here should characterize maser radiation once the source is sufficiently large that the radiation field is dominated by emission along the longest chords. These polarization properties are easy to understand: In the case of π-components, the generated electric field oscillates along the magnetic field lines. Therefore, whatever the viewing angle, the polarization is always purely linear, parallel to the magnetic axis. The intensity vanishes as the propagation direction approaches the magnetic axis, on account of the transverse condition. In the case of σ-components, the generated electric field describes a circle in the plane perpendicular to the magnetic axis. For propagation along the field lines ($\theta = 0$) the circle is viewed face-on and the polarization is purely circular ($Q = U = 0$). For propagation at an oblique angle to the field the circle is viewed in projection and the polarization is elliptical. Finally, the ellipse degenerates to a line for propagation perpendicular to the field ($\theta = \pi/2$), since the circle is viewed edge-on. The polarization is then linear, perpendicular to the magnetic field lines.

5. OVERLAPPING ZEEMAN COMPONENTS: $g\nu_B \ll \Delta\nu$

When $g\nu_B$ exceeds all particle interaction rates yet is smaller then the line width (GKK's case 2), the magnetic substates can be considered quantized along a common axis, but the frequencies of the various Zeeman components coincide. Radiation is generated with electric components along all three B-frame axes at the same frequency. For each wave, these components of the electric field are related to the k-frame components through the inverse of equations (2.4):

$$\begin{aligned} E^x &= E_x \cos\theta - E_z \sin\theta , \\ E^y &= E_y , \\ E^z &= E_x \sin\theta + E_z \cos\theta . \end{aligned} \tag{5.1}$$

The waves that propagate in the medium are transverse, i.e., $E_z = 0$. Now, insert this condition in equations (5.1), transform to circular B-components, calculate complex absolute values, and perform ensemble averages as prescribed by the definitions of the Stokes parameters. The result is

$$\begin{aligned} I^{+1} &= \tfrac{1}{4}[I(1+\cos^2\theta) - Q\sin^2\theta + 2V\cos\theta] , \\ I^{-1} &= \tfrac{1}{4}[I(1+\cos^2\theta) - Q\sin^2\theta - 2V\cos\theta] , \\ I^0 &= \tfrac{1}{2}(I+Q)\sin^2\theta . \end{aligned} \tag{5.2}$$

The intensity components I^p obtained this way are the ensemble-averaged intensities of waves that propagate in the medium in steady state, and thus correspond to the transverse radiation field that exists in the source. Equations (5.2) show that these quantities are entirely equivalent to the three Stokes parameters I, Q, and V. Therefore, except for the parameter U, the Stokes parameters can be specified in terms of pure intensities. At any frequency across the line and every point in the source and for propagation in any direction, the polarization state of the radiation field can be described using either the four Stokes parameters or, equivalently, the three intensity components I^p and the Stokes parameter U. The latter parameter does not couple to the level population equations with the choice of axes made here, and it can be noted that it remained undetermined in the GKK solution. As shown below, the symmetry of the problem implies that $U = 0$ for the overall radiation field.

From the left-right symmetry,

$$I^{-1} = I^{+1} \equiv I^1 , \tag{5.3}$$

and equations (5.2) show that $V = 0$ under these circumstances. The circular polarization vanishes, and only linear polarization is possible in this case. A straightforward inversion of equations (5.2) then produces

$$\frac{Q}{I} = -1 + \frac{2}{\sin^2\theta(1 + 2I^1/I^0)} . \tag{5.4}$$

The linear polarization is determined completely by the ratio of the two intensity components, and every solution for Q/I can be expressed in this form with the proper choice of I^1/I^0. For example, unpolarized radiation corresponds to

$$\frac{2I^1}{I^0} = \frac{1+\cos^2\theta}{\sin^2\theta} . \tag{5.5}$$

As is evident from the results of the previous section, such an intensity ratio can be obtained from the radiation of independent, equal-intensity $\Delta m = 0$ and $|\Delta m| = 1$ masers in a magnetic field emitting at the same frequency.

Since the polarization parameters cannot exceed the overall intensity, the relation $-I \le Q \le I$ must always be obeyed. As evident from equation (5.4), the condition $Q/I \ge -1$ is trivially met, while the requirement $Q/I \le 1$ implies that

$$I^0 \le 2I^1 \tan^2\theta . \tag{5.6}$$

The intensity component I^0 is always constrained by this relation, that is, radiation propagating at a direction close to the quantization axis cannot contain too high an intensity in its $p = 0$ state. This constraint, equivalent to $Q/I \le 1$, is evidently a consequence of the transverse condition.

Consider now an arbitrary position inside the maser, assuming that the source is sufficiently large that the radiation is beamed. The direction of the dominant ray is determined purely by the geometry; it is simply the direction of the longest chord through the source, and is thus the same for both $p = 0$ and $p = 1$. As before, the intensity components $I^p(\mu_0)$ ($p = 0, 1$) of the dominant ray at a given frequency are expected to be determined by the pump and loss mechanisms at that frequency. Suppose that the θ-independent particle interactions produce these intensities at the ratio $\mathcal{R}_{01}$, namely,

$$I^0(\mu_0) = \mathcal{R}_{01} I^1(\mu_0) . \tag{5.7}$$

Because of the transverse condition (eq. [5.6]), this relation can hold only so long as $\theta \ge \theta_B$, where θ_B is determined from

$$\tan^2\theta_B = \mathcal{R}_{01}/2 . \tag{5.8}$$

For propagation closer to the quantization axis, i.e., $\theta \le \theta_B$, only waves whose intensity $I^0(\mu_0)$ obeys the transverse condition (5.6) can contribute to the dominant ray at steady state. Waves that obey both the equality and inequality signs will propagate, but those that obey the equality sign will obviously dominate the intensity. As a result,

$$I^0(\mu_0) = I^1(\mu_0) \times \begin{cases} \mathcal{R}_{01} , & \theta \ge \theta_B , \\ 2\tan^2\theta , & \theta \le \theta_B , \end{cases} \tag{5.9}$$

and the polarization of dominant rays is

$$\frac{Q}{I} = \begin{cases} -1 + \dfrac{2}{\sin^2\theta(1 + 2/\mathscr{R}_{01})}, & \theta \geq \theta_B, \\ 1, & \theta \leq \theta_B. \end{cases} \quad (5.10)$$

The polarization changes its functional form at a certain angle, in agreement with previous studies that derived solutions for specific models (GKK; Litvak 1975; Western & Watson 1984). This break is simply dictated by the requirement that the polarization not be more than complete, equivalent to the transverse condition.

When $\mathscr{R}_{01} = 1$,

$$\tan^2\theta_B = \tfrac{1}{2}, \quad \text{i.e.,} \quad \sin^2\theta_B = \tfrac{1}{3}, \quad (5.11)$$

and the polarization of dominant rays is

$$\frac{Q}{I} = \begin{cases} \dfrac{2 - 3\sin^2\theta}{3\sin^2\theta}, & \theta \geq \theta_B, \\ 1, & \theta \leq \theta_B. \end{cases} \quad (5.12)$$

This can be immediately recognized as the GKK solution for $J = 1 \rightarrow 0$ saturated masers with isotropic pumping, i.e., m-independent pump and loss rates. The analysis in terms of B-frame intensity components shows that this solution simply describes the polarization of beamed maser radiation for any spin and any degree of saturation when the pumping processes establish $I^0(\mu_0) = I^1(\mu_0)$ for dominant rays sufficiently removed from the magnetic axis. The generalization of the GKK solution to arbitrary pump rates is provided by equation (5.10).

As in the case $\mathscr{g}v_B \gg \Delta v$, the polarization properties can be further understood from an analysis of the structure of the electric fields of propagating waves. Consider again an arbitrary position inside the maser, assuming that the source is sufficiently large that the radiation is beamed. From equations (5.2) a measurement of the Stokes parameters of the radiation propagating in any direction at a given frequency provides the corresponding intensity components, in particular the components $I^p(\mu_0)$ $(p = 0, 1)$ of the dominant ray. Define again the real amplitudes $E^p = [I^p(\mu_0)/\mathscr{K}]^{1/2}$; then the complex amplitudes of any propagating wave that can contribute to the main beam are obtained through multiplication by arbitrary phases. Denote the phase of the $p = 0$ amplitude by b and the shifts from it of the $p = \pm 1$ amplitudes by $\varphi^{\pm}$. The three B-frame components of the electric fields of waves in the main beam are then

$$E^0 e^{ib}, \quad E^+ = E^1 e^{i(b+\varphi^+)}, \quad E^- = E^1 e^{i(b+\varphi^-)}. \quad (5.13)$$

The k-frame components of the wave's electric field are obtained by inserting these amplitudes into equations (2.4). In the resulting linear combinations, the common phase e^{ib} is simply an overall multiplicative factor. Temporarily removing it for clarity, the k-frame complex amplitudes are

$$\begin{aligned} E_x &= 2^{-1/2}E^1(e^{i\varphi^+} + e^{i\varphi^-})\cos\theta + E^0\sin\theta, \\ E_y &= -i2^{-1/2}E^1(e^{i\varphi^+} - e^{i\varphi^-}), \\ E_z &= -2^{-1/2}E^1(e^{i\varphi^+} + e^{i\varphi^-})\sin\theta + E^0\cos\theta. \end{aligned} \quad (5.14)$$

Any wave launched in the main beam can be described by these amplitudes when the overall common random phase e^{ib} is reinstated. However, only waves whose electric field is perpendicular to the direction of the dominant ray will propagate. The propagating waves are identified from the multitude of launched waves by selecting those that obey the transverse condition $E_z = 0$. This is a complex equation, providing two constraints on the phase differences $\varphi^{\pm}$. The imaginary part implies that $\sin\varphi^+ + \sin\varphi^- = 0$, or

$$-\varphi^+ = \varphi^- \equiv \varphi; \quad (5.15)$$

this phase relation ensures the removal of circular polarization. The magnitude of the phase φ is then determined from the real part of the constraint:

$$\cos\varphi = \frac{E^0}{2^{1/2}E^1\tan\theta}. \quad (5.16)$$

This determines the magnitude of φ but not its sign, and both $+\varphi$ and $-\varphi$ are equally valid. Because we seek to identify only waves that propagate in steady state, the phase φ must be real. Therefore, $\cos^2\varphi \leq 1$—the transverse condition of equation (5.6).

With the phase differences that ensure transverse structure determined, the overall phase e^{ib} can be reinstated and the observed (k-frame) components of the electric fields of propagating waves in the main beam are

$$\begin{aligned} E_x &= 2^{1/2}E^1e^{ib}\cos\varphi/\cos\theta = E^0e^{ib}/\sin\theta, \\ E_y &= 2^{1/2}E^1e^{ib}\sin\varphi \\ &= \pm e^{ib}[2(E^1\sin\theta)^2 - (E^0\cos\theta)^2]^{1/2}/\sin\theta. \end{aligned} \quad (5.17)$$

As before, the Stokes parameters of dominant rays are obtained at once from the definitions in equations (2.1) after ensemble-averaging over these waves. The result is

$$\begin{aligned} I &= 2I^1 + I^0, \\ Q &= -(2I^1 + I^0) + 2I^0/\sin^2\theta, \\ U &= \pm(2/\sin\theta)[2I^1I^0 - (I^0/\tan\theta)^2]^{1/2}, \\ V &= 0. \end{aligned} \quad (5.18)$$

The intensity components obtained from these Stokes parameters with the aid of equations (5.2) reproduce the quantities $I^p(\mu_0)$ we started with, verifying the consistency of the construction.

The results show that waves propagating in steady state along dominant rays belong to two families of solutions—the normal modes of the problem. In either mode the waves are 100% linearly polarized ($Q^2 + U^2 = I^2$) and have the same values of I and Q. Equivalently, the two modes have the same intensities I_x and I_y of radiation whose polarization is, respectively, in the plane of the magnetic axis and perpendicular to it:

$$\begin{aligned} I_x &= I^0/\sin^2\theta, \\ I_y &= 2I^1 - I^0/\tan^2\theta. \end{aligned} \quad (5.19)$$

The difference between the modes is in the opposite sign of the parameter U. For each wave, this parameter is directly related to the polarization position angle $\chi = \frac{1}{2}\tan^{-1}(U/Q)$, which is simply the azimuthal angle $\tan^{-1}(E_y/E_x)$ in this case. It is thus determined from

$$\tan\chi = \pm(\cos\theta)(2I^1\tan^2\theta/I^0 - 1)^{1/2}. \quad (5.20)$$

For any wave belonging to one of the normal modes there is a corresponding one in the other mode obtained through mirror reflection about the ***k*-*B*** plane. The two modes evolve indepen-

dently because the difference between them is the parameter U, which does not couple to particle interactions. Every arbitrary linear polarization state can be prepared as an appropriate admixture of waves in the two modes. While all admixtures are allowed in principle, the two faces of the $\boldsymbol{k}$-$\boldsymbol{B}$ plane are equivalent, so only admixtures of equal amounts can be considered relevant for actual sources, and the parameter U vanishes for the overall radiation field.

The polarization properties of the dominant rays are determined by the independent pumping of magnetic sublevels. Radiation is produced incoherently in three different p-states whose electric fields oscillate along three independent axes. From this multitude of waves, the only ones that will propagate in the direction of the local dominant ray are those whose overall electric field is perpendicular to that direction, so the three components must be reduced to two. This reduction occurs only for waves that were launched with the proper relations among the phase differences of the three components of the field (the overall phase is still arbitrary). These waves, and only these waves, will propagate. When the propagation direction approaches the magnetic axis, phase differences alone are insufficient to produce transverse combinations; this is evident from the fact that at $\theta = \theta_B$ the phase difference φ, and the position angle χ, vanish, the two normal modes collapse to one, and the electric field perpendicular to the $\boldsymbol{k}$-$\boldsymbol{B}$ plane vanishes too. The transverse condition requires now that for propagating waves, the amplitudes of the p-states, not merely their phases, be related to each other. Thus the propagating waves are fully polarized, but the intensity of the radiation field is reduced continuously from $2I^1 + I^0$ at $\theta = \theta_B$ to $2I^1$ at $\theta = 0$. The solution formally shows that the radiation is fully polarized even for propagation exactly along the field lines ($\theta = 0$), although in this case the geometry does not define any direction perpendicular to the field that could define the sense of polarization. This is obviously a singular configuration because the $\boldsymbol{k}$-$\boldsymbol{B}$ plane cannot be defined, and averaging over all azimuthal directions shows that the polarization vanishes. This trivial singularity is removed once the propagation direction and magnetic axis are not perfectly aligned, and the radiation is then fully polarized. In addition, because the intensity $I^0(\mu_0)$ is suppressed, its beaming will be less prominent close to the magnetic axis. The implications of this effect can only be studied in specific geometrical models.

Similar to the $g\nu_B \gg \Delta\nu$ case, the radiative transfer equations for the intensity components of the dominant rays, $I^p(\mu_0)$, can be obtained by inserting the electric fields from equations (5.17) into the general result of equation (3.4). Following the same standard steps, the results of equations (4.6) are recovered in this case too. Again, radiative transfer for the dominant rays is determined by the radiative interaction terms in the level population equations once the radiation is beamed, and the dominant rays diagonalize the equations of radiative transfer. As, before, the polarization properties emerge once beaming provides an adequate description for the radiation field.

5.1. *Isotropic Pumping*

We can now complete the solution of isotropic pumping for masers of arbitrary spins. This case corresponds to equal pump and loss rates for the magnetic substates of each level. Additionally, the standard assumption of equal loss rates for the two levels ($\Gamma_a = \Gamma_b \equiv \Gamma$) is also made; this is not essential, but it simplifies the expressions. The magnetic subscripts can then be deleted in the level population equations (3.1), and the population differences obey

$$P_a - P_b = \Gamma(n_{am} - n_{bn}) + 3g_a B_{ab}\Big[\sum_{p,k} J^p c_p(a, m; b, k) \times (n_{am} - n_{bk}) + \sum_{p,k} J^p c_p(a, k; b, n)(n_{ak} - n_{bn})\Big] . \quad (5.21)$$

When the maser is saturated, the radiative terms can be neglected on the right-hand side, and the population difference is the same for each pair (m, n), namely,

$$n_{am} - n_{bn} = n_a - n_b . \quad (5.22)$$

As a result, with the aid of the normalization relation for the c-coefficients (eq. [3.2]), the absorption coefficients for the two B-frame intensity modes are equal, and

$$\kappa^1 = \kappa^0 = \kappa , \quad (5.23)$$

where κ is the standard expression for the absorption coefficient of the $a \rightarrow b$ line (eq. [4.6]). In other words the component intensities of the dominant rays $I^0(\mu_0)$ and $I^1(\mu_0)$ grow at the same rate. They are therefore equal to each other, and thus

$$\mathscr{R}_{01} = 1 . \quad (5.24)$$

Because the intensity components grow at the same rate, they also saturate at the same position inside the maser. Once the maser is saturated, the dominant-ray intensities $I^p(\mu_0)$ grow in proportion to the difference in pump rates of the maser levels. Because the pump rates are m-independent, the intensities continue to grow at the same rate in the saturated regime as well, and equations (5.22)–(5.24) hold irrespective of the degree of saturation.

The same conclusion can be reached using a somewhat more formal, mathematical argument. The left-hand side of equation (5.21) is independent of m and n, while the dependence on these indices of the right-hand side enters only in different, additive terms. The equation is invariant when each of these indices is held fixed while the other is varied at will. The only possible solution is equal populations among the magnetic sublevels of each state. This is a fairly obvious result, considering the assumption of m-independent pump and loss rates. As before, the equations of radiative transfer for the dominant rays become p-independent, and the intensity components grow at the same rate. The population difference is therefore

$$n_a - n_b = \frac{P_a - P_b}{\Gamma + B_{ab} J(g_a + g_b)/g_b} , \quad (5.25)$$

which for $g_a = g_b$ reverts to the standard result for a two-level scalar system (§ 3).

The result $\mathscr{R}_{01} = 1$ reflects the assumption of equal pump and loss rates for all sublevels, which tend to produce the same intensity in all transitions, and completes the solution of the problem. The explicit expressions for the polarization properties of beamed radiation are listed in equations (5.11)–(5.12). Figure 2 displays the variations of the polarization Q/I and the magnitudes of the phase difference φ and the position angle χ as functions of θ.

As in the case $g\nu_B \gg \Delta\nu$, the results are in complete accord with the GKK solution procedure, which analyzed the behavior of the matrix $\boldsymbol{R}$ for the Stokes parameters. In the unsaturated regime, $\boldsymbol{R}$ is diagonal for isotropic pumping (eq. [64] in GKK), in agreement with equations (4.6). In the saturated domain, GKK again required that the polarization approach a

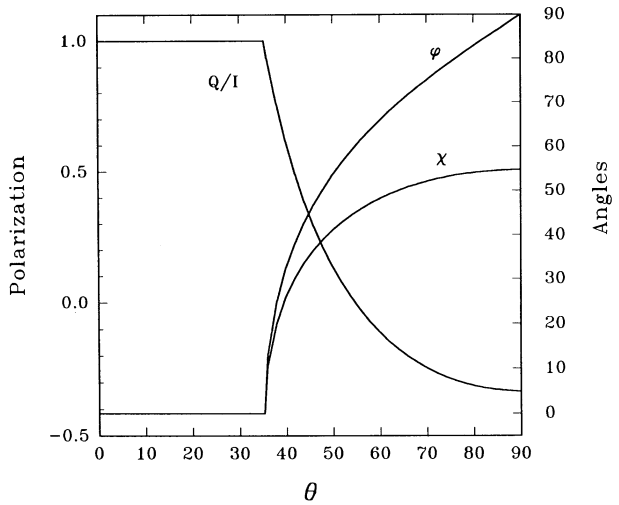

FIG. 2.—Isotropic pumping polarization as a function of direction of the dominant ray from the *B*-axis. The scale on the left is for the polarization curve, marked with Q/I. The scale on the right is for the magnitudes of the two angles that characterize the polarization normal modes: φ, the phase difference between $\Delta m = 0$ and $|\Delta m| = 1$ electric fields, and χ, the position angle.

limit, equivalent to the requirement that $\boldsymbol{R}$ become diagonal for the dominant rays, as shown here. In fact, the diagonalization technique employed by GKK even utilized the intensity components $I^p(\mu_0)$, and their solution is in complete agreement with the one derived here. As before, the present results provide an explicit construction of the GKK solution. The stability analysis performed in that paper thus provides additional, formal proof for the stability of this solution, a point obvious from the *B*-frame construction presented here. The GKK analysis identified an additional solution (eq. [61] in that paper), shown to be unstable. This solution contains circular polarization, and its instability stems from the conflict with the left-right symmetry of the pump rates. Mode switching to this solution will occur when the pump rates for two of the *p*-states are turned off, which is how the $g\nu_B \ll \Delta\nu$ solution transforms into the one for $g\nu_B \gg \Delta\nu$.

In the unsaturated regime, $\boldsymbol{R}$ is identically diagonal, and any polarization state is amplified unchanged. Because of the lack of constraint stemming from the diagonalization procedure, GKK concluded that the radiation is unpolarized. However, it should be noted that this conclusion was actually never proved; such a proof requires a demonstration that $Q^2 + U^2 + V^2 = 0$, and this was never done. In fact, the level population equations show that, whatever the degree of saturation, in steady state the intensity components I^p are equal to each other, and the polarization solution follows. This is evident also from equations (23) of GKK, where the radiative interaction rates $B_{ab} I^p$ are denoted $U_{a_p a_p}$. It may also be noted that the GKK radiative transfer equations are consistent with equation (2.2) and $Q\,dQ + U\,dU + V\,dV = I\,dI$ in all cases, for both saturated and unsaturated masers, as should be the case. Therefore, applying the GKK radiative transfer equations to a configuration belonging to one of the normal modes and evolving it along a dominant ray from the saturated regime toward lower intensities properly produces unsaturated beamed radiation with the same polarization.

The GKK technique was employed by Western & Watson (1984) and Deguchi, Watson, & Western (1986) for the study of $J = 1 \rightarrow 0$ and $2 \rightarrow 1$ systems. These studies show that the GKK limit solution applies also to $J = 2 \rightarrow 1$ masers, in agreement with the results derived here. However, the numerical calculations presented in these papers had great difficulties in approaching this polarization solution. The limit was essentially never attained for $J = 2 \rightarrow 1$ masers, and in the case of $J = 1 \rightarrow 0$ it was approached only at extreme intensities. These difficulties can be traced to the initial conditions and source terms employed in the numerical studies. The assumption of equal populations in steady state equilibrium with propagating plane waves requires that the waves be polarized according to the GKK solution for propagation in any direction. Instead, the numerical calculations were started with different intensities that led to an internal conflict that is most evident from the expressions for the source terms (eqs. [4] and [6] of Deguchi et al.). These terms generate radiation polarized parallel to the $\boldsymbol{k}$-$\boldsymbol{B}$ plane through a perfectly correlated emission of $\Delta m = 0$ and $|\Delta m| = 1$ photons at a predetermined, angle-dependent mixture. Such emission conflicts with the assumption of incoherent pump processes and leads to an internal inconsistency: On the one hand, the level population equations drive the solution toward equal populations and equal-intensity components $I^p(\mu_0)$—the GKK limit solution, as properly recognized by Deguchi et al. in the discussion preceding their equation (32). On the other hand, the intensities generated by the source terms produce the contradictory result that $I^0 = I^1$ corresponds to unpolarized radiation. It may be noted that initial intensities consistent with steady state level populations would have led to the polarization solution in the numerical calculations. The transport of radiation polarized according to the GKK solution by the transfer equations of Deguchi et al. produces equal amplification for both intensities, and the polarization is unaffected by radiative transfer.

In conclusion, the polarization of dominant rays in an isotropically pumped maser source is determined by the radiation generation processes and is unaffected by the subsequent effects of radiative transfer because the various Stokes parameters grow at the same rate. The dominant rays' polarization is identical in this case in the saturated and unsaturated regimes, and the GKK limit procedure provides one method for identifying it.

5.2. *Anisotropic Pumping*

In the case of *m*-dependent pumps, the intensity components of the dominant rays obey

$$\frac{d[I^1(\mu_0)/I^0(\mu_0)]}{dl} = (\kappa^1 - \kappa^0)\left[\frac{I^1(\mu_0)}{I^0(\mu_0)}\right], \qquad (5.26)$$

as is evident from equation (4.6), so this is the relation that determines the variation of the polarization in the source (cf. eq. [5.4]). This relation again shows that radiative transfer has no effect on the dominant rays' polarization in the case of isotropic pumping (where $\kappa^1 = \kappa^0$). When both radiative modes are saturated, they both grow with the same power of distance traveled, and the ratio $I^1(\mu_0)/I^0(\mu_0)$ becomes l-independent. Therefore, the absorption coefficients for both modes must then be the same, which is indeed the case: The absorption coefficient of a long saturated maser is α/l, where α is a geometry-dependent coefficient and l is the length traveled along the dominant-ray path in the saturated zone, independent of mode properties (Elitzur 1990). Therefore, *dominant-ray maser polarization will always approach a limit in the saturated domain.* The value of this limit polarization is determined solely by the ratio of pump rates for the two *p*-modes.

The full solution for m-dependent pump rates is straightforward, but the results tend to become involved. Expressions relevant for the completely general case were worked out by Litvak (1975). For simplicity we consider here only a $J = 1 \rightarrow 0$ system. The c-coefficients are then the same for all transitions, $c_p = \frac{1}{3}$, and there is just one B-coefficient. The two levels are assumed to have the same loss rate Γ, so the two modes are described by a single saturation intensity $J_s = \Gamma/(2B)$. The pump rate into the lower level is P_0; those into the $m = 0$ and $m = \pm 1$ substates of the upper level are P_{10} and P_{11}, respectively. The requirement that all transitions be inverted implies $P_{1p} > P_0$ ($p = 0, 1$). A straightforward solution of the level population equations shows that the absorption coefficients for the two p-states are

$$\kappa^0 = \frac{\kappa_0^0 + (3\kappa_0^0 - 2\kappa_0^1)J^1/J_s}{1 + (2J^0 + 3J^1)/J_s + 4J^0 J^1/J_s^2},$$

$$\kappa^1 = \frac{\kappa_0^1 + (2\kappa_0^1 - \kappa_0^0)J^0/J_s}{1 + (2J^0 + 3J^1)/J_s + 4J^0 J^1/J_s^2}, \quad (5.27)$$

where κ_0^p denote the respective unsaturated absorption coefficients. These coefficients have the form $\kappa_0^p = \text{const} \times (P_{1p} - P_0)/\Gamma$, and their ratio q is therefore

$$q \equiv \frac{\kappa_0^0}{\kappa_0^1} = \frac{P_{10} - P_0}{P_{11} - P_0}. \quad (5.28)$$

The ratio of the two source functions is then $P_{10}/(qP_{11})$. In an unsaturated maser, the intensity of each p-state away from the edge is $S^p \exp(\kappa_0^p l)$; thus the unsaturated variation of $\mathscr{R}_{01}$ is

$$\mathscr{R}_{01} = \frac{S^0}{S^1} \exp[(\kappa_0^0 - \kappa_0^1)l] = \frac{P_{10}}{qP_{11}} \exp[\kappa_0^1 l(q - 1)]. \quad (5.29)$$

When the two modes saturate ($J^p > J_s$), their absorption coefficients become

$$\kappa_s^0 = \tfrac{1}{4}(3\kappa_0^0 - 2\kappa_0^1)J_s/J^0, \quad \kappa_s^1 = \tfrac{1}{4}(2\kappa_0^1 - \kappa_0^0)J_s/J^1, \quad (5.30)$$

and the radiative transfer equation for the dominant ray of each p-state contains the ratio $I^p(\mu_0)/J^p$, the radiation beaming factor. With the same beaming for both p-states, the intensity ratio in the saturated regime becomes

$$\mathscr{R}_{01} = \frac{3\kappa_0^0 - 2\kappa_0^1}{2\kappa_0^1 - \kappa_0^0} = \frac{3P_{10} - 2P_{11} - P_0}{2P_{11} - P_{10} - P_0}. \quad (5.31)$$

The two expressions derived for $\mathscr{R}_{01}$ (eqs. [5.29] and [5.31] complete the solution in the unsaturated and saturated regimes, respectively. The polarization in each regime is obtained upon insertion in equations (5.8) and (5.10). The unsaturated polarization varies toward the saturated limit, and the variation rate depends on the specific values of the loss and three pump rates. Since both p-states were assumed to mase, the pump rates are constrained by the requirement that both κ_s^0 and κ_s^1 be positive. This restricts the pump rates to the range

$$\tfrac{2}{3} < q < 2. \quad (5.32)$$

The constraint arises because the intensities of the two p-states are coupled through their effect on the level populations in the saturated regime, a coupling best illustrated by the detailed expressions for the absorption coefficients (eq. [5.27]). The case $q = 1$ corresponds to isotropic pumping ($P_{10} = P_{11}$). It is evident that, in this case, $\mathscr{R}_{01} = 1$ in both the saturated and unsaturated domains, and the solution of the previous section is recovered.

5.3. *Interaction with Streams*

Although the calculations were performed assuming that the state quantization was induced by a magnetic field, the specific properties of the magnetic interaction never entered. Once the magnetic axis can be considered a good quantization axis, the matrix elements of the magnetic interaction are diagonal in the quantum number m, and they do not induce any transitions; their only effect is to shift the energies of various states. Thus the only relevant property is the introduction of a good quantization axis for the entire source. But this can be done by other mechanisms as well, in particular interaction with a stream of either particles or photons. Because the properties of the interaction that causes space quantization never enter the calculation, the results apply to this situation as well. The pump rates are usually m-dependent in this case, so the anisotropic solution is the relevant one. The polarization is always linear, because the left-right symmetry cannot be broken.

An example of such a mechanism is Johnston's (1967) electron stream collisions for OH excitations. In this model, $\Delta m = 0$ transitions are the only ones with rates that are larger in the upward direction; thus only I^0 intensity is generated as maser radiation. This case does not conform to the above analysis because the $p = 1$ mode does not mase and condition (5.32) is not obeyed. However, this situation is identical to that in π-components of a fully developed Zeeman pattern, so $Q = I$. Formally, the same solution can also be obtained from the relations listed here with $\mathscr{R}_{01} \rightarrow \infty$, i.e., $\theta_B = \pi/2$. Indeed, Figure 2 of Johnston's paper shows that maser action is produced only for polarization parallel to the direction of the stream (the other polarization never produces a negative absorption coefficient), in agreement with the results derived here.

6. SUMMARY AND DISCUSSION

The results derived here show that the GKK solutions for $J = 1 \rightarrow 0$ masers hold independent of spins or degree of saturation for the polarization of the dominant rays in sources with sufficient amplification that the radiation is beamed. When $\mathscr{g}\nu_B \ll \Delta\nu$, GKK provided the solution only for isotropic pumping, and equation (5.10) provides the simple generalization for other types of pumps. The solutions require that the magnetic axis can be considered a good quantization axis, so that the sublevels are quantized with respect to it. The appropriate condition is given in equation (1.1). This also ensures that the gyro-rate $\mathscr{g}\omega_B$ exceeds Γ, the maser loss rate. In principle the self-interaction of the maser molecules with the maser radiation they generate could destroy state quantization and depolarize the radiation. However, for an unsaturated maser equation (1.1) ensures that the interaction rate with maser radiation BJ is smaller than the gyro-rate, so this does not happen. When the maser radiation reaches the saturated domain, it is already properly polarized and the radiative interactions maintain this polarization, even when BJ exceeds the gyro-rate.

It is importat to emphasize that the results depend in a crucial manner on the assumption of a constant direction for the magnetic field throughout the source. Any curvature in the field lines would introduce a variable θ, and the radiation propagating from one region to another would arrive with the

wrong phase relations for that particular region, thus destroying some polarization. Therefore, the solutions derived here provide the maximal polarization that can be produced in a source; field-line curvature would reduce the degree of polarization. The polarization may also be reduced by the effects of Faraday rotation, which were neglected here. Those were listed in GKK and can be simply added to the results, in the manner described in that paper.

Net polarization can also be produced when an overall quantization axis is provided by an interaction with a stream. The situation is similar to that of magnetic fields with $g\nu_B \ll \Delta\nu$, and only linear polarization is produced. The generation of circular polarization requires removal of the degeneracy of magnetic substates. Except for nonlinear effects that can be neglected in astronomical masers, there is no known mechanism yet for generating circular polarization other than magnetic interaction with fields strong enough that $g\nu_B > \Delta\nu$. The detection of such polarization can thus be taken as an indication of the field strength in the source. This is of particular relevance to the recent measurements of circular polarizations in SiO (Barvainis, McIntosh, & Predmore 1987) and OH (Cohen et al. 1987) maser radiation in late-type stars. The interpretation proposed in these papers in terms of strong magnetic fields (up to ~ 100 G at the stellar surface) is corroborated. It is also interesting to note that the OH circular polarization was detected in particularly narrow spectral features (Cohen et al.), indicating that the high degrees of field alignment and velocity coherence may be correlated in these sources.

The overall interpretation of polarization observations is similar to that of the previous studies. By and large, OH masers follow the predictions of the Zeeman solution ($g\nu_B \gg \Delta\nu$), while SiO and H_2O polarizations conform to the $g\nu_B \ll \Delta\nu$ case. It is important to note that the information that can be extracted from polarization alone is limited because the same polarization can usually be produced in a number of different ways. For example, OH emission from H II regions displays in general a high degree of circular polarization with occasional linear polarization, as expected from a paramagnetic molecule with $g\nu_B > \Delta\nu$ (which for OH requires $B \gtrsim 10^{-3}$ G for a line width of 1 km s^{-1}). However, the source OH 48.6+0.0 displays only high linear polarization, 29% and 68% in two spectral components, without any circular polarization (Evans et al. 1979). This could be explained in a number of ways. First, the magnetic field could be so weak in this source that $g\nu_B < \Delta\nu$ and the Zeeman pattern does not develop. This is certainly possible, although somewhat unlikely in view of the fact that in most other H II/OH regions circular polarization is detected. If this explanation is rejected, there are still two possibilities: For some reason, we may be detecting only the π-components from this source. Again, this would make this an exceptional source. Finally, the magnetic field could simply lie in the plane of the sky so that the detected radiation always travels perpendicular to the field lines, producing only linear polarization. This appears to be the most likely explanation, but there is no reason to prefer it from polarization measurements alone. Similarly, when a linear polarization of less than 100% is observed in an SiO or H_2O maser source, it can be attributed either to the maximal polarization at an appropriate angle θ or to a higher polarization that was degraded by curvature in the field lines.

A major departure from conclusions of earlier studies involves the minimal fields required to produce linear polarization in SiO and H_2O masers. As shown here, propagating plane waves in equilibrium with steady state level populations are polarized according to the GKK solution for propagation in any direction and any degree of saturation. How these modes are selected for amplification from the isotropic, background radiation generated by spontaneous decays remains an open problem. However, assuming that the steady state equilibrium modes dominate the maser radiation field, the requirement of equation (1.1) suffices to produce net linear polarization. The most restrictive condition then is $g\omega_B > A$ with the appropriate A-coefficient (corresponding to rotational and vibrational transitions for H_2O and SiO, respectively). Thus, the production of linear polarization in either case necessitates field strengths in excess of only $\sim 10^{-4}$ to 10^{-5} G. Such fields are most certainly readily available in the sources, and the linear polarization finds a simple explanation. The fact that H_2O masers display in general a somewhat lower polarization than SiO masers can be attributed to the conditions at the emission region. In late-type stars, the SiO emission originates from cells close to the stellar surface (Elitzur 1980), where the motions may be correlated with the structure of the magnetic field. This can provide an alignment of the field lines throughout each velocity-coherent cell corresponding to a maser feature, resulting in relatively high polarizations. In contrast, the H_2O maser radiation is generated in the expanding shell around the star at a position where the wind still accelerates. The angular extent of the emission region,

$$\theta_e \simeq (d \ln v / d \ln r)^{1/2} \tag{6.1}$$

(Elitzur, Goldreich, & Scoville 1976), is relatively large and can contain many field lines pointing in different directions, so the polarization averages out. In the case of H_2O masers in star-forming regions, in all likelihood these occur behind high-velocity shocks (Elitzur, Hollenbach, & McKee 1989). The polarization is then less than maximal because Alfvén waves can wiggle the field lines, thus reducing the polarization. It is interesting to note in this respect that the strong H_2O maser outburst in Orion distinguished itself also with very high linear polarization (up to $\sim 70\%$; Garay, Moran, & Haschick 1989). Thus the burst event may be associated with a field alignment.

As in previous works, maser polarization was studied here in only two distinct limits, corresponding to Zeeman components that either fully separate ($g\nu_B \gg \Delta\nu$) or completely overlap ($g\nu_B \ll \Delta\nu$). The transition between these extremes is an unsolved problem whose importance is underscored by the recent observations of Cohen et al. (1987) and Zell & Fix (1990). These provide evidence for sharp reversals in the profile of the Stokes parameter V (which measures net circular polarization)—a clear signature of magnetic fields with $g\nu_B \sim \Delta\nu$, intermediate between the two available solutions. In spite of its importance, the $g\nu_B \sim \Delta\nu$ case remains unsolved. The analysis of this paper points to phase interference between electric fields generated in various Δm transitions as the key to the solution. Work on this problem is in progress.

Finally, although the focus of this study is on maser radiation, it shows that an analysis in terms of the intensity components I^p can be a powerful tool that provides valuable insight for polarization properties in general. This approach could prove useful for study of ordinary, nonmaser line radiation. Polarization of ordinary radio lines in molecular clouds has been analyzed in a number of studies in recent years, and the B-frame approach developed here could prove advantageous in this case too.

I am greatly indebted to M. M. Litvak for illuminating discussions that helped elucidate and clarify many of the issues discussed here. In addition, I thank T. H. Troland for useful comments on the manuscript. This work was begun during a visit to the Weizmann Institute of Science, Rehovot, Israel. The hospitality of the Department of Nuclear Physics is gratefully acknowledged, as is the support of NSF grant AST-8716936.

REFERENCES

Barvainis, R., McIntosh, G., & Predmore, C. R. 1987, Nature 329, 613
Cohen, R. J., et al. 1987, MNRAS, 225, 491
Deguchi, S., Watson, W. D., & Western, L. R. 1986, ApJ, 302, 108
Elitzur, M. 1980, ApJ, 240, 553
———. 1982, RevMoPhy, 54, 1225
———. 1990, ApJ, 363, 638
Elitzur, M., Goldreich, P., & Scoville, N. 1976, ApJ, 205, 384
Elitzur, M., Hollenbach, D. J., & McKee, C. F. 1989, ApJ, 346, 983
Evans, N. J., Beckwith, S., Brown, R. L., & Gilmore, W. 1979, ApJ, 227, 450
Garay, G., Moran, J. M., & Haschick, A. D. 1989, ApJ, 338, 244
Goldreich, P., Keeley, D. A., & Kwan, J. Y. 1973a, ApJ, 179, 111 (GKK)
———. 1973b, ApJ, 182, 55
Johnston, I. D. 1967, ApJ, 150, 33
Litvak, M. M. 1970, PhyRv, A2, 2107
———. 1975, ApJ, 202, 58
Messiah, A. 1961, Quantum Mechanics (Amsterdam: North-Holland)
Moran, J. M. 1989, in Molecular Astrophysics, ed. T. Hartquist (Cambridge: Cambridge Univ. Press), in press
Reid, M. J., & Moran, J. M. 1981, ARAA, 19, 231
Sargent, M., Lamb, W. E., & Fork, R. L. 1967, PhyRv, 164, 436
van de Hulst, H. C. 1957, Light Scattering by Small Particles (New York: Wiley)
Western, L. R., & Watson, W. D. 1984, ApJ, 285, 158
Zell, P. J., & Fix, J. D. 1990, preprint